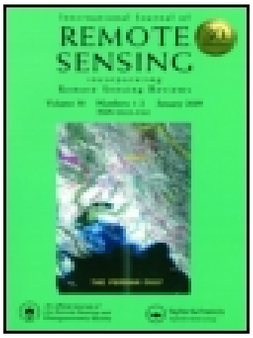

International Journal of Remote Sensing

ISSN: 0143-1161 (Print) 1366-5901 (Online) Journal homepage: http://www.tandfonline.com/loi/tres20

Annual anomalies and trends for TOMS reflectivities (1978–2005) in the Southern Hemisphere

Adrián E. Yuchechen, S. Gabriela Lakkis & Pablo O. Canziani

To cite this article: Adrián E. Yuchechen, S. Gabriela Lakkis & Pablo O. Canziani (2017) Annual anomalies and trends for TOMS reflectivities (1978–2005) in the Southern Hemisphere, International Journal of Remote Sensing, 38:12, 3483-3501, DOI: 10.1080/01431161.2017.1294778

To link to this article: http://dx.doi.org/10.1080/01431161.2017.1294778

INTERNATIONAL JOURNAL OF REMOTE SENSING, 2017
VOL. 38, NO. 12, 3483–3501
http://dx.doi.org/10.1080/01431161.2017.1294778

Annual anomalies and trends for TOMS reflectivities (1978–2005) in the Southern Hemisphere

Adrián E. Yuchechen [a], S. Gabriela Lakkis [b,c] and Pablo O. Canziani [a]

[a]Universidad Tecnológica Nacional (UTN), Facultad Regional Buenos Aires (FRBA), Consejo Nacional de Investigaciones Científicas y Técnicas (CONICET), Unidad de Investigación y Desarrollo de las Ingenierías (UIDI), Buenos Aires, Argentina; [b]UTN, FRBA, UIDI, Buenos Aires, Argentina; [c]Pontificia Universidad Católica Argentina, Facultad de Ingeniería y Ciencias Agrarias, Buenos Aires, Argentina

ABSTRACT

Annual anomalies of Lambertian equivalent reflectivity (LER) retrieved from the total ozone mapping spectrometer spanning the period November 1978–November 2005 were studied in the Southern Hemisphere, in a region bounded by 0° S and 60° S, and their trends were estimated. With the exception of few regions where the variable may represent the contribution of both cloudiness and snow, trends in LER anomalies provided an evolution of total cloudiness. On average, the study region experienced a net increase in LER values of 0.78 reflectivity units (RU) decade^{-1}; if only significant trend values are considered this figure increased to 1.18 RU decade^{-1}. The region that showed the largest upward trend, up to 4 RU decade^{-1}, was located over the eastern Pacific, off the coasts of Chile and Peru, where the presence of marine stratocumulus is frequent. Despite the overall positive trend there were regions that yielded a negative one, most notably the tropical latitudes of South America and Africa. The yearly zonal means also showed a positive trend at all latitudes, but significance occurred beyond 20° S only. Correlation maps between LER anomalies and five different circulation indices were also introduced. The indices with the highest and lowest number of significant correlation values were the Madden–Julian oscillation at 70° E and the quasi-biennial Oscillation, respectively.

ARTICLE HISTORY
Received 13 June 2016
Accepted 31 January 2017

1. Introduction

The advent of global warming and climate change scenarios increasingly require observations of the climate system and its forcings so as to properly address them (Kondratyev and Varotsos 1995). Cloud cover, ice extent, and their radiation budget are among the many components of the climate system that requires a far better understanding. They are also highly relevant because of their strong influence on the biological cycles, particularly on the aquatic and the terrestrial ecosystems (Häder et al. 2003; Bornman et al. 2015). Changes in the radiation budget of incoming solar radiation

CONTACT Adrián E. Yuchechen aeyuchechen@frba.utn.edu.ar Unidad de Investigación y Desarrollo de las Ingenierías, Facultad Regional Buenos Aires, Universidad Tecnológica Nacional, Mozart 2300 (C1407IVT), Buenos Aires, Argentina

Supplemental data for this article can be accessed here.

(ISR) in the near-ultraviolet, the visible, and the near-infrared wavelengths, as well as of outgoing emitted radiation at infrared wavelengths are at least partly linked to variations in the cloud cover (Herman et al. 2013). Cloud distribution is considered part of a feedback mechanism that directly impacts global warming (Boucher et al. 2013). The primary role played by clouds is linked to the Earth's heat budget, which relies upon the imbalance of the ISR and the space-bound outgoing longwave radiation. Simply stated, low and thick clouds primarily reflect the ISR and cool the Earth's surface, whereas the ISR is transmitted by high and thin clouds and they simultaneously trap some of the outgoing infrared radiation emitted by the Earth and re-radiate it downwards, thereby warming the Earth's surface. In addition, on long-time scales clouds are recognized to play a strong influence in climate, whereas on short-time scales they induce the exchange of heat between cloudy and clear-sky regions (Stowe et al. 1989, and references therein).

A proper assessment of climate projections requires a complete understanding of the feedback between radiation, clouds and aerosols (Boucher et al. 2013). In general, reported changes for clouds are strongly related to cloud amount and their geographical distribution. Geometrical and physical properties are usually disregarded. Eastman and Warren (2013) found that the global cloudiness had an overall decline of 0.4% per decade for the period 1971–2009 and that different regional trends occurred if this value was broken down by continent. In particular, South America had a negative trend of 1.4% per decade, and a value of −0.5% per decade was found for Australia and the Pacific Islands. They also reported a global negative trend in cloud anomalies over the oceans up to 2000 and a reversion of the trend from then on. Furthermore, Trenberth and Fasullo (2009) asserted that a significant surface warming is expected during the ongoing century owing to a negative trend in global cloud cover. The authors predicted a decreasing trend in both Hemispheres for low and mid clouds over mid-latitudes and of high clouds around the Equator, with the negative trend showing a strengthening in the second half of the century in all these cases; in contrast, an increase of total cloud cover with enhanced trends in the second half of the century is expected over the poles.

Changes in cloud cover caused by natural low frequency fluctuations in circulation patterns of the atmosphere and oceans (i.e. El Niño/Southern Oscillation (ENSO, Philander 1989), the North Atlantic Oscillation (Lamb and Peppler 1987), the Pacific Decadal Oscillation (PDO, Mantua et al. 1997), or the dipole mode index (DMI, Saji et al. 1999)) may modulate the climate system's radiative balance and therefore lead to inaccurate conclusions regarding global warming (Spencer and Braswell 2008, 2011). To this respect, it is necessary to take into account the possible linkages between two or more of the aforementioned circulation patterns (e.g. Kidson 1999; Varotsos 2013). As a matter of fact, Saji et al. (1999) mentioned independence between the DMI and the ENSO, whereas an ENSO/PDO relation was highlighted by Mantua et al. (1997).

Previous studies (e.g. Cess and Udelhofen 2003; Norris 2005) analysed trends based on cloud fraction information derived from visible and infrared wavelengths using the International Satellite Cloud Climatology Project database (Rossow and Schiffer 1999, and references therein) and the Extended Edited Cloud Report Archive surface observations database (Hahn and Warren 1999). There exist different ways to evaluate the radiation budget and its variability, yet an accurate evaluation requires high quality ground-based observations. Unfortunately, these are mostly recent, scant, and non-

uniformly distributed nor performed over the globe (Liang et al. 2010; Varotsos et al. 2014). In particular, few ground-based time series in the Southern Hemisphere (SH) have records exceeding a decade (Damiani et al. 2014), so satellite observations render as an important supplementary tool to monitor radiation and its variability in both regional and global scales (Von Schuckmann et al. 2016).

The Lambertian equivalent reflectivity (LER) of the Earth's surface and atmosphere provides valuable information on ultraviolet (UV) reflectivity from the oceans and land, as well as that from clouds and atmospheric aerosols. LER is a quantitative measure of the total amount of energy reflected from the Earth back to space in sunlight. It represents the average reflectivity of a combination scene that includes the contribution from clouds, the Earth's surface and airborne aerosols, neglecting multiple Rayleigh scattering effects, and under the assumption that all the reflecting surfaces behave as an ideal Lambertian reflector (Labow et al. 2011; Den Outer et al. 2012).

LER values range from 0 to 1 yet they are usually expressed in reflectivity units (RU), ranging from 0 to 100 (e.g. Herman et al. 2009, 2013). Primarily related to ozone, LER is also useful as a cloudiness proxy (Labow et al. 2011; Herman et al. 2013) as well as for snow cover assessments (Herman and Celarier 1997). LER cannot provide disaggregated information of cloud types and amount of aerosol contributions, but it is suitable for detecting changes in regional and global cloud reflectivity amounts considering that in the absence of snow and ice the lowest UV surface reflectivity is nearly constant in time both for land and water (Herman and Celarier 1997). The accuracy of continuous long-term records from instruments aboard different satellites can be considered comparable to time series from ground-based instruments, making remotely-sensed information valuable in studies where measuring radiation reflected back to space can be relevant (e.g. Buchard et al. 2008; Damiani et al. 2014).

The goal of this work is to provide a first analysis of annual LER distribution and trends over the SH within the 0° S–60° S latitudinal band together with an assessment of the relationship between LER variability and known major tropical and extra-tropical circulation variability processes such as the ENSO, the PDO and the DMI, among others, for the period November 1978–November 2005. To the best of our knowledge, this study is the first of its kind that completely devotes such an analysis to the SH. This first research effort is restricted to Total Ozone Mapping Spectrometer (TOMS) data retrieved during the Nimbus-7 (N7) and the Earth Probe (EP) missions.

2. Data and methodology

The present analysis includes TOMS LER retrievals collected by two different satellites between November 1978 and November 2005. LER monthly mean values were obtained from the National Aeronautics and Space Administration's Atmospheric Composition Data and Information Service Centre (ACDISC), available at ftp://acdisc.gsfc.nasa.gov/data/s4pa/. Daily LER data reprocessed using the Version 8 algorithm was available for the TOMS instruments aboard the N7, the Meteor-3 (M3) and the EP satellite missions; they spanned the period November 1978–April 1993, August 1991–November 1994 and July 1996–November 2005, respectively. In all cases, daily data was mapped to a grid from 89.5° N to 89.5° S and from 179.375° W to 179.375° E with a resolution of 1° and 1.25°, respectively. The available daily LER values at ACDISC involved the measurements

made at each mission's reference channel, which was the longest wavelength insensitive to ozone absorption, i.e. 380 nm (N7 and M3) and 360 nm (EP). Further technical details regarding the three satellite missions – such as the calculation of daily LER values at each pixel – can be found in the work of Herman et al. (1996), McPeters et al. (1996), and McPeters et al. (1998). LER monthly means for the N7 and EP missions were also available at the ACDISC database, but they were not available for the M3 campaign. The data's geographical spacing for the monthly means matched the one for daily data. Some issues related to the degradation of the scan mirror (EP) and to photomultiplier detector hysteresis effects (N7) (Herman et al. 2013) do not seem to compromise the use of LER values as a cloudiness proxy, since the two databases are consistent with ground-based measurements (Den Outer et al. 2012; Damiani et al. 2014).

The Ozone Measuring Instrument (OMI) database followed the TOMS one. It has been providing a number of TOMS-like remotely-sensed products, 360-nm LER in particular (Ozone Monitoring Instrument (OMI) Algorithm Theoretical Basis Document 2002), since the Aura satellite, on board which the OMI is flown, was launched in 2004 (Ozone Monitoring Instrument (OMI) User's Guide 2012). Many research efforts employed both overlapping databases (e.g. Herman et al. 2009; Pinedo Vega et al. 2014). However, for this first stage we decided not to merge the information coming from the two datasets. The study we carried out here will be expanded with the inclusion of OMI data in a separate paper (manuscript in preparation).

Annual means were calculated from the monthly values at each pixel within the November 1978–November 2005 timespan. Mean values for M3 were not calculated in order to avoid the possible introduction of differences with any algorithm used by the TOMS Science Team, so the LER monthly mean values used in this research corresponded to the ones readily obtainable from the ACDISC database, i.e. the N7 (1978–1993) and the EP (1996–2005) missions. TOMS data was retrieved for daylight conditions regardless of the solar zenith angle (unlike the retrieval of data from instruments aboard zenith-angle-limited satellites, e.g. the Sea-viewing Wide Field-of-view Sensor (McClain et al. 2000)) so there are missing LER values for the winter months at latitudes beyond the Arctic and the Antarctic circles, i.e. during the polar night. In this respect, even though the estimation of least-square annual trends is valid within the 70° N–70° S belt (Herman et al. 2009), the study region in the SH was limited to the latitudinal band from the Equator and 60° S in order to avoid the inclusion of missing values due to this effect. Both the grand-time means and the standard deviations were also calculated. At each pixel, the former was subtracted from the annual mean in order to obtain LER anomalies fields. They were tested for significance using a 95% confidence level following Hoel (1984, 288–291).

3. Results

Figures 1(*a*) and (*b*) show the grand-time mean and the standard deviations, respectively. Figure 1(*a*) includes surface albedoes (Herman and Celarier 1997) superimposed to values associated to cloudiness and aerosols, and to specific snow-covered regions. In general, the dependence with latitude shows a distinct behaviour north and south of 30° S. Aside from regional departures, on average LER takes on lower values north of this latitude at all longitudes with the exception of those around 60° W, where a tongue of

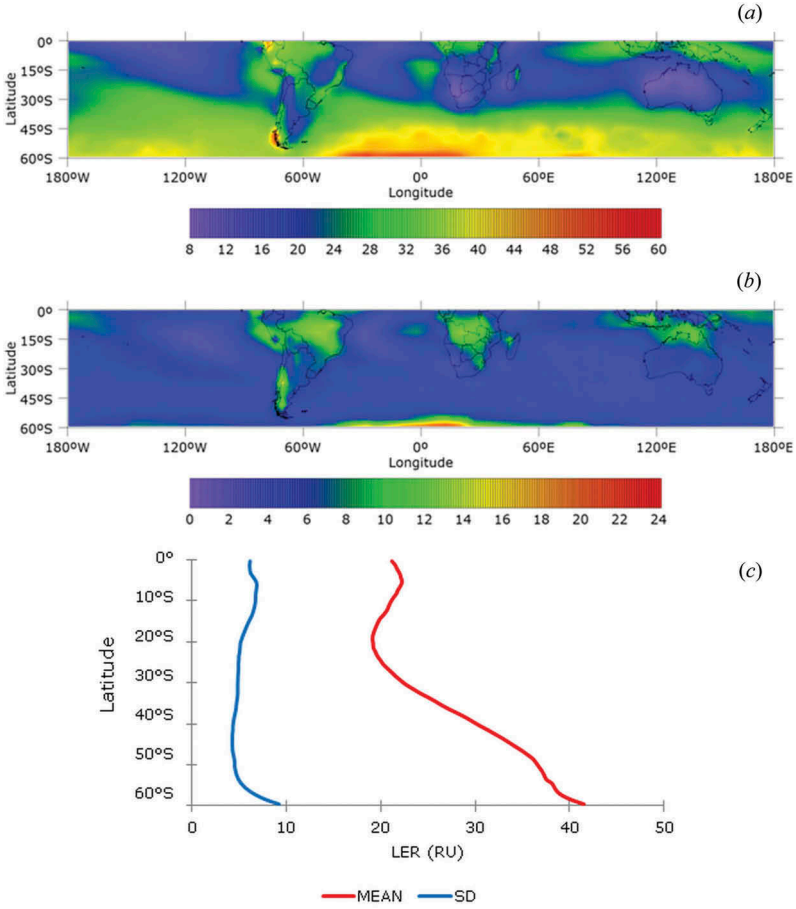

Figure 1. LER grand-time means and standard deviations (in RU) for the entire period of analysis: (*a*) mean values; (*b*) standard deviations (SD); (*c*) zonal means of the quantities shown in (*a*) and (*b*).

lower values relative to its surroundings extend down to approximately 55° S. At low latitudes, the regions with relative higher LER values generally occur over landmasses. The northwestern portion of South America, with LER values slightly over 40, can be associated either with cloudiness or with permanent or semi-permanent snow (e.g. the elevation of the Chimborazo volcano in Ecuador is over 6200 m (Schoterer et al. 2003)). Relative higher values over northeastern South America, western equatorial Africa (spanning Gabon, the Republic of the Congo and the Democratic Republic of the Congo, from west to east), the western Indian Ocean (IO) off the coast of Indonesia and the austral portions of Indonesia and Malaysia, and over Papua New Guinea and adjacent waters, are all related to cloudiness in agreement with Eck et al. (1987). Another feature that is properly depicted is the relative higher values off the Peruvian coast that are tied to the presence of marine stratocumulus (Kuang and Yung 2000). Similarly, the resemblance between the Humboldt and the Benguela currents, in that both flow northwards, parallel to the coastline, and within the eastern flank of a semi-permanent anticyclone, suggests the local higher values in the South Atlantic, off the coasts of

Namibia and Angola, are also attributable to stratocumulus' persistence. The lowest values associated with least overcast regions year-round, in particular those located in the descending branch of the Hadley cell, such as the Kalahari desert (Stokes et al. 1998) or northwestern Australia (Ashkenazy, Yizhaq, and Tsoar 2012), are also visible.

Two items at latitudes beyond 30° S are worth noting. One of them is the relative greater values (of around 50 RU) approximately along 50° S, in a region approximately bounded by 60° W and 40° E, that may be related to year-round storm track activity (Hoskins and Hodges 2005); these values have a marked zonal asymmetry that is in line with earlier findings (Inatsu and Hoskins 2004). The other peculiarity is the contrast in LER values over the southern Andes. A possible explanation for this relies upon topography-generated waves in the region (Eckermann and Preusse 1999), where synoptic systems crossing the mountain range act as a forcing for the development of such perturbations (Nappo 2002), leading to the formation of clouds with different characteristics on both sides of the mountains with a yield on LER values. When the LER variability is considered, stable background LER values associated to albedos of permanent surface features vanish in Figure 1(*b*). It is worth noting that the low-latitude regions having the highest variabilities are, in general, shifted approximately 10° south of the equatorial ones having the greater means. These largest fluctuations, generally located over landmasses, can be associated, for example, with the variable occurrence of different cloud tops (Eck et al. 1987). Another high-variability region lies on the coastal waters of Peru (tied to stratocumulus variability). The regions with the highest variability are the southern Andes (this can be associated either with convection and varying dynamics or with snow cover variability) and the South Atlantic at the lowest latitudes in the domain, around the Greenwich Meridian. On the other hand, lesser variability occurs over the oceans. Figure 1(*c*) shows LER zonal means. Generally speaking, mean reflectivities increase southwards from values above 20 RU at the tropics up to ones above 40 RU at the highest latitudes, with an absolute minimum (LER values below 20 RU) at approximately 20° S, in coincidence with the descending branch of the Hadley cell (Herman et al. 2013). The greatest reflectivities at the southernmost latitudes are caused by clouds over ice-free waters (Labow et al. 2011). In general, zonal variability follows the behaviour of the zonal mean. It ranges from slightly over 4 RU up to approximately 9 RU, with maximum values taking place at the southernmost latitudes and associated to the above-mentioned storm tracks.

Figure S1 (supplemental data) shows an animation for yearly anomaly fields. Significant values are also marked. The grand-time variances considered are the square of the values in Figure 1(*b*). At each pixel the variances from year to year were assumed to be different from the grand-time variance so an annual variance was also calculated. Only two different representative years in Figure S1 will be discussed. One of them is the loop's first map for 1978. It accounted for seasonality since it shows anomalies for November-December only (i.e. late spring/early summer in the SH). Seasonal characteristics are also included in the 1993, 1996, and 2005 maps. An entire year whose anomalies will be discussed is 1983 due to the ENSO effect.

As to 1978, positive anomalies occurred in 51% of the cases (ignoring 453 grid-points with missing values), with less than a fifth of the domain having significant differences. The percentages of positive and negative values for each year, as well similar figures for significant and not significant differences are further discussed below. The most visible

significant positive anomalies during this year occurred over Africa and South America around 15° S, whereas significant negative differences were recorded mostly over the oceans, yet southern South America and Western Australia were also affected by such anomalies.

One of the best known, yet not completely understood, phenomena that couples the atmosphere and the oceans and affects the large-scale circulation is the ENSO. One way to estimate the phase the system is in (i.e. either an ENSO warm or cold event for El Niño and La Niña, respectively, or else neutral conditions) relies upon the Southern Oscillation Index (SOI), which is related to the difference of pressures between Tahiti and Darwin (Ropelewski and Jones 1987). Negative (positive) values are an indication of a warm (cold) event, whereas, broadly speaking, the closest the SOI is to zero the more undistorted are the conditions in the atmosphere/ocean system considering solely this phenomenon. The SOI time series both in plain anomalies and in a standardized version are available at the National Oceanic and Atmospheric Administration/National Weather Service's Centre for Weather and Climate Prediction – Climate Prediction Centre (CPC) (http://www.cpc.ncep.noaa.gov/data/indices/soi). Both 1982 and 1983 were marked by an ENSO warm event (Philander 1989, 38). According to the CPC database, the strongest stage of this event took place between January and February 1983. Furthermore, the SOI index had negative values in half of this year's months, with the most negative ones spanning from January to April. Given that ENSO warms events are characterized by a shift of the Walker cell (i.e. a migration of convection) from the western to the central equatorial Pacific (Peixoto and Oort 1992, 412–449), the loop's panel for 1983 seems to be representing the first months of this year reasonably well, with anomalies at the latter region being significant and positive. On average, an apparent local strengthening of Yasunari's (1977) wavenumber-4 pattern took place only in the Atlantic region during this year, in resemblance with the non-canonical relation between ENSO warm events and the increase in the amount of precipitation along the South Atlantic Convergence Zone (Ambrizzi, De Souza, and Pulwarty 2004).

One way to address the relationships between the loop's panels relies upon the Pearson's correlation coefficient r with a pixel-by-pixel calculation. Nevertheless, this mixes up significant values with no significant ones. In order to take into account only significant anomalies the correlations were carried out including only those grid-points whose values from the pair of correlated maps were both significant. The greater the absolute value of r the higher the correspondence between regions sharing significant anomalies. Both the correlations between the loop's maps and the number of paired grid-points with significant values included in the calculations are shown in Table 1. For 1983, the absolute value attained by r with all the previous years maximized at 1982 with a value of 0.73, sharing 207 grid-points. Spatially, these results basically owe their existence to the persistence of positive anomalies in spots over equatorial latitudes in the Pacific and of negative anomalies over the three oceans at mid-latitudes. Figure S2 (supplemental data) includes an animation that shows the location of the points with significant differences shared by the pair of years indicated that maximized the absolute value of r.

Figures 2(*a*) and (*b*) show the percentages of positive and negative differences and the percentages of significant and not significant values, respectively, for each year. Two distinct periods can clearly be identified from Figure 2(*a*): the first one between 1978

Table 1. Matrix composition showing the Pearson's correlation coefficients (right triangular matrix) between the significant grid-points in the anomalies maps of Figure S1 (supplemental data) and the number of grid-points included in these calculations (left triangular matrix).

	1978	1979	1980	1981	1982	1983	1984	1985	1986	1987	1988	1989	1990	1991	1992
1978	–	0.69*	0.16	−0.05	−0.36*	−0.32	−0.12	−0.09	−0.21	0.04	−0.10	−0.07	−0.05	−0.07	−0.38
1979	106*	–	0.92*	0.74	−0.24	−0.57	−0.64	0.02	−0.39	−0.05	−0.61	−0.65	0.26	0.63	0.14
1980	147	70*	–	0.94*	0.30	−0.29	−0.80*	−0.39	0.34	0.39	−0.73*	−0.56	0.12	0.71	0.21
1981	222	53	97*	–	0.31	−0.13	0.02	−0.07	0.13	0.04	0.01	−0.11	0.23	−0.38	−0.18
1982	215*	44	84	63	–	0.73*	−0.27	0.17	0.78*	0.74*	−0.53	−0.16	0.78	0.67	−0.10
1983	478	132	192	162	207*	–	0.16	0.26	0.38	0.57	0.13	0.24	0.60	−0.69	0.66
1984	328	103	215*	218	245	310	–	0.73*	0.23	−0.60	0.67	0.70	0.00	−0.73	−0.83*
1985	501	137	221	213	264	494	537*	–	0.70	−0.68	0.69	0.83*	0.24	0.34	−0.66
1986	524	131	221	212	365*	528	420	654	–	0.01	0.33	0.75	0.83*	0.37	−0.70
1987	397	113	285	153	213*	467	428	420	551	–	−0.46	−0.76	0.26	0.69	0.73
1988	355	136	202*	142	111	389	348	395	427	318	–	0.68	0.29	−0.74	−0.45
1989	354	119	241	135	103	328	371	559*	492	345	492	–	0.27	−0.74*	−0.78
1990	396	60	117	139	205	301	327	305	395*	440	310	301	–	0.48	0.05
1991	137	41	90	26	112	111	103	121	135	188	59	60*	85	–	0.47
1992	190	71	89	94	87	154	232*	273	228	422	195	270	111	121	–
1993	148	67	107	62	84	177	160	179	170	225	155	196	89	80	353*
1994	–	–	–	–	–	–	–	–	–	–	–	–	–	–	–
1995	–	–	–	–	–	–	–	–	–	–	–	–	–	–	–
1996	424	84	201	147	203*	398	323	441	447	392	261	308	264	74	240
1997	281	63	193	169	132	253	292	393	351	318*	246	319	214	32	97
1998	378	113	227	166	150	320	264	393	360	387	223	261	213	162*	203
1999	310	106	280	153	191	328	409	403	394	796	318	462	246	175*	253
2000	274	135	249	199	211	415	403	462	305	811	303	402	244	147*	302
2001	148	33	88	68	75	127	166	214	218	220	161	161	132	54	79
2002	323	83	124	131	183	279	295*	377	319	338	234	322	200	113	237
2003	364	117	219	190	244	391*	314	428	466	368	298	267	314	80	134
2004	376	117	221	206	302	436*	567	488	566	397	369	383	348	80	155
2005	611	152	248	308	428	490*	561	740	798	460	345	363	383	149	197

Diagonal values and those including years 1994 and 1995 (both with missing monthly means in the original database) are omitted.
*Values related to the maps shown in Figure S2 (supplemental data); the associated correlation coefficients are significant to a 95% confidence level.

Table 1. Continued.

	1993	1994	1995	1996	1997	1998	1999	2000	2001	2002	2003	2004	2005
1978	-0.23	–	–	0.55	-0.01	-0.30	-0.23	-0.06	0.12	0.19	0.25	0.25	0.26
1979	0.41	–	–	0.09	-0.35	-0.71	-0.80	-0.84	0.42	0.59	0.56	0.69	0.40
1980	0.70	–	–	-0.53	0.16	-0.73	-0.86	-0.80	-0.35	0.64	0.26	0.35	0.23
1981	-0.44	–	–	-0.45	-0.42	-0.49	-0.54	-0.30	0.03	-0.36	-0.13	-0.25	-0.23
1982	-0.03	–	–	-0.75*	0.66	-0.47	-0.30	-0.56	-0.89	0.37	-0.62	-0.57	-0.47
1983	0.02	–	–	-0.57	0.60	0.83	-0.22	-0.62	-0.90	-0.75	-0.94*	-0.85*	-0.89*
1984	-0.81	–	–	0.48	-0.48	0.58	0.75	0.71	0.45	-0.76*	-0.27	-0.26	-0.23
1985	-0.69	–	–	0.55	-0.45	0.09	0.72	0.71	0.44	-0.45	0.23	0.23	0.01
1986	-0.38	–	–	-0.45	-0.39	-0.27	0.46	0.42	0.44	0.36	0.19	0.19	0.05
1987	0.78	–	–	-0.69	0.82*	0.13	-0.88	-0.94	-0.70	0.37	-0.42	-0.72	-0.48
1988	-0.69	–	–	0.42	-0.20	0.65	0.88	0.73	-0.21	-0.47	-0.35	-0.30	-0.25
1989	-0.80	–	–	0.72	-0.50	0.37	0.81	0.84	0.19	-0.50	0.13	-0.06	-0.16
1990	0.14	–	–	-0.07	-0.13	0.33	0.14	-0.40	-0.27	-0.10	-0.06	-0.10	-0.03
1991	0.77	–	–	-0.67	0.06	-0.90*	-0.92*	-0.97*	-0.19	0.37	0.47	0.66	0.39
1992	0.98*	–	–	-0.28	0.77	-0.01	-0.85	-0.86	-0.63	0.12	-0.31	0.15	-0.19
1993	–	–	–	-0.47	0.43	-0.48	-0.91	-0.87	-0.38	0.21	0.22	0.50	0.16
1994	–	–	–	–	–	–	–	–	–	–	–	–	–
1995	–	–	–	–	–	–	–	–	–	–	–	–	–
1996	126	–	–	–	-0.73	-0.10	0.82	0.90	0.85	-0.04	0.84	0.66	0.63
1997	142	–	–	302	–	0.49	-0.75	-0.74	-0.85	0.49	-0.72	-0.75	-0.62
1998	159	–	–	325	203	–	0.39	0.13	-0.50	-0.59	-0.76	-0.63	-0.71
1999	213	–	–	277	293	342	–	0.97	0.65	-0.38	-0.11	-0.08	-0.09
2000	225	–	–	342	329	397	711	–	0.94*	-0.39	0.20	0.05	0.11
2001	66	–	–	132	150	121	192	138*	–	0.36	0.82	0.83	0.82
2002	133	–	–	234	183	238	268	315	98	–	0.76	0.57	0.27
2003	101	–	–	328	310	271	222	288	148	337	–	0.80	0.81
2004	110	–	–	405	283	310	305	422	162	401	583	–	0.65
2005	143	–	–	584	353	502	308	525	248	459	721	997	–

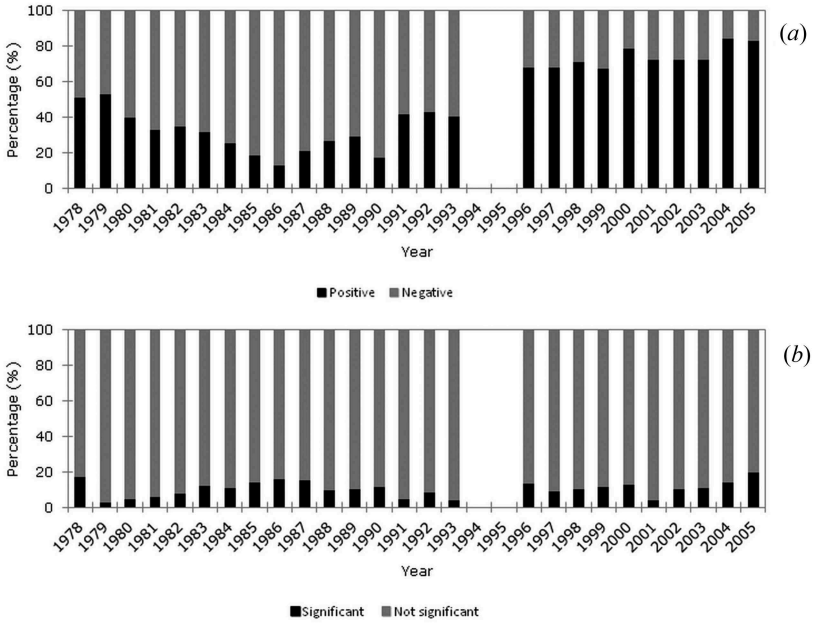

Figure 2. Breakdown of percentages for the differences shown in the panels of Figure S1 by year: (*a*) positive and negative; (*b*) significant and not significant.

and 1993 with a majority of negative anomalies, and the second one between 1996 and 2005 at which there was a dominance of positive anomalies. The average percentages for positive values are 33% and 74% for the former and the latter, respectively. The minimum and maximum percentages of positive values took place in 1986 (13%) and 2004 (85%), respectively. An upward trend for positive values is noticeable since 1986. McPeters et al. (1998) noted a small positive trend of approximately 0.5 RU in LER values in the first 1.5 years of operation of the EP mission. Assuming this trend as steady from 1996 onwards, it represents, at worst, a spurious increase of 3% in the LER values at the end of the second period. The difference in the percentages of positive values between 2005 and 1996 is well above 3% so there are no reasons for not to treat the observed changes as real. By contrast, Figure 2(*b*) shows no apparent differences in the number of significant points for the two periods. On average, these figures are 10% (12%) for the first (second) period; the maximum percentage (20%) occurred in 2005 and the minimum one took place in 1979 (3%). Disregarding the pixel or the region, this big picture outlines a general upward trend for the differences but not for their significance.

In order to provide further insights on individual regions, Figure 3 shows the trend for the yearly anomalies at each pixel (i.e. the trend for the values shown in Figure S1). Positive trends dominated, and negative trends were generally not significant. The strongest significant positive trends over the tropical eastern Pacific, off the coast of Chile and Peru with values up to 4 RU decade^{-1}, contrast with the non-significant trends in the western equatorial Pacific, and may be an indication of a strengthening of ENSO events during the period of analysis. For the 1980–1992 timespan, Herman et al. (2009) too found a net increase in LER values off the coast of Chile and Peru and attributed it to changes in the cloud cover caused by variations in the Humboldt Current (HC). The

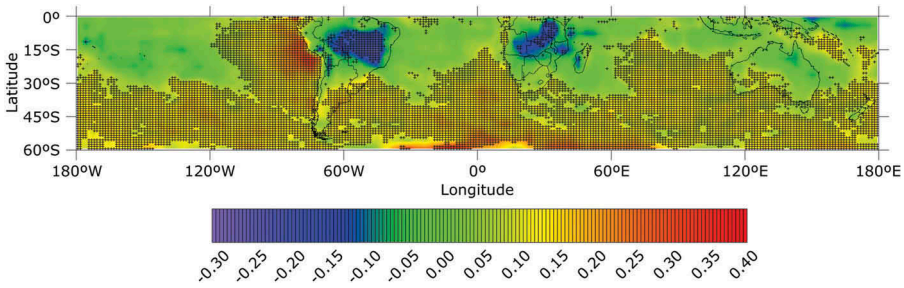

Figure 3. Trends (in RU year^{-1}) for the anomalies shown in Figure S1. Significant values at a 95% confidence level are cross-hatched.

assessment of an ENSO/HC connection is beyond the scope of the present work. However, reflectivity on a yearly basis does not show a clear relationship between them since during the two strong ENSO warm events that took place in the analysed period, represented by the positive anomalies in the central equatorial Pacific in 1983 and 1998, anomalies of opposite sign for each of these two years occurred in the Pacific coast of tropical and subtropical South America (cf. Figure S1).

There is another region with moderate to strong significant positive trends along 60° S, from 15° W to 75° E, that may be related to higher storm track activity. The 30° S–45° S band had significant trends almost all over the oceans. North of 30° S significant trends were found in the western coasts of the landmasses only. The zonal means of the values shown in Figure S1 have positive trends everywhere with significance from 20° S down to the southernmost limit of the domain (results not shown). These results are in contradiction with those presented by Eastman and Warren (2013) but they employed sparse information over the oceans. On average, the entire SH showed a positive trend of 0.78 RU decade^{-1} disregarding significance; if only significant values are considered (9680 pixels out of 17,280, or 56% of the domain) the trend raises to 1.18 RU decade^{-1}. Both figures indicate that most of the pixels in the SH exhibited an upward trend. Notwithstanding, there were regions that had an opposite behaviour. They accounted for just 3% of the total number of pixels with significant values. Negative trends were found over the equatorial portions of eastern Africa and eastern South America, in agreement with Eastman and Warren (2013) who found downward trends over the same regions for the period 1971–2009. They also found a negative trend over north-eastern Australia. Such trends were also found here but they were not significant. In general, the trends' regional features found here are qualitatively matched by the ones presented in Herman et al. (2013, cf. Figure 13).

In order to present the spatial patterns of reflectivity associated to global atmospheric phenomena on a yearly basis, Figures 4(*a*)–(*n*) show the Spearman's correlation coefficient ρ between yearly anomalies of LER and of five atmospheric indices known for being related to phenomena with impacts on the global circulation. Unlike r that accounts for linear relationships between the variables, ρ acts on the ranks of the variables (Wilks 2006), so it is more suitable to establish a relationship between the variables through a monotonic function, not necessarily linear, that links them. The indices included in this analysis are the DMI (monthly means retrieved from http://www.jamstec.go.jp/frcgc/research/d1/iod/DATA/dmi.monthly.txt), the PDO (monthly

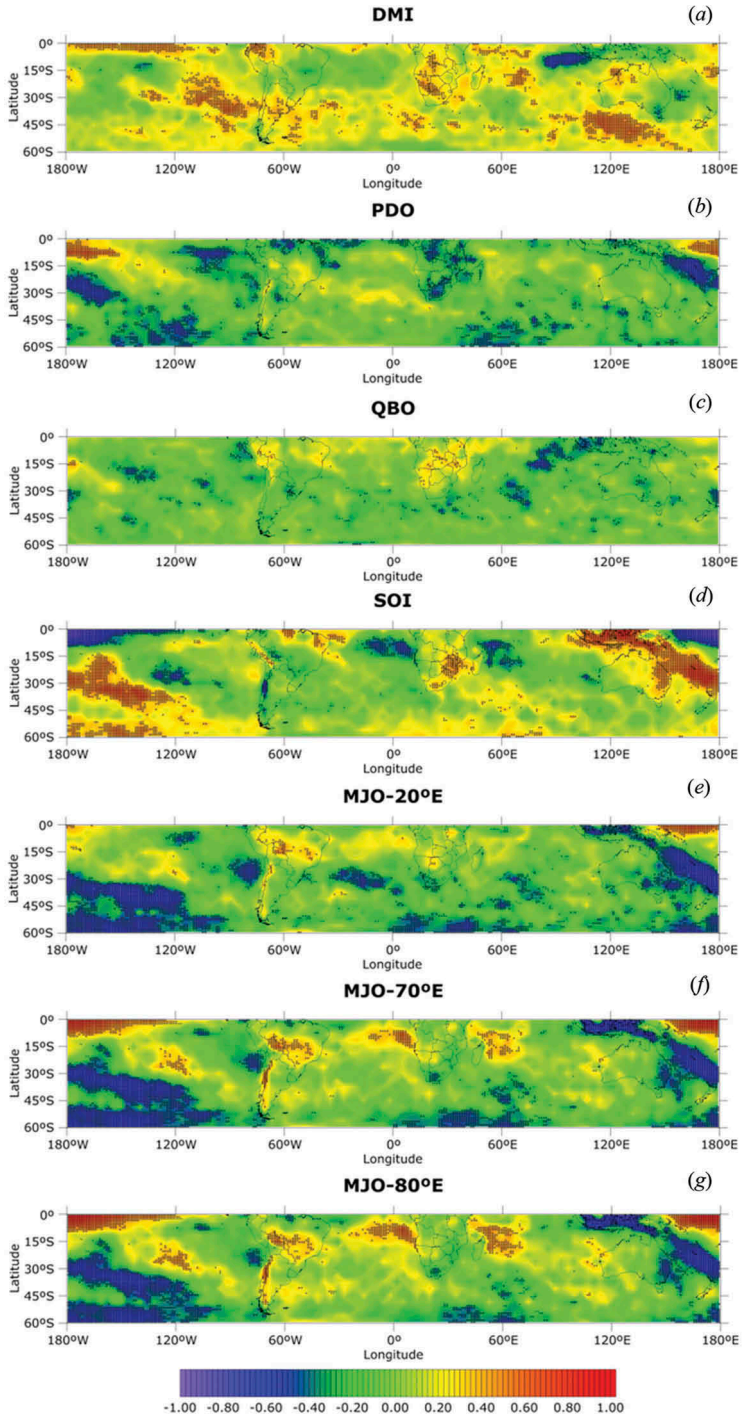

Figure 4. Spearman's correlation coefficients between yearly anomalies of LER and those of five atmospheric circulation indices: (*a*) DMI; (*b*) PDO; (*c*) QBO; (*d*) SOI; (*e*)–(*n*) MJO from 20° E to 10° W. Significant values at a 95% confidence level are cross-hatched.

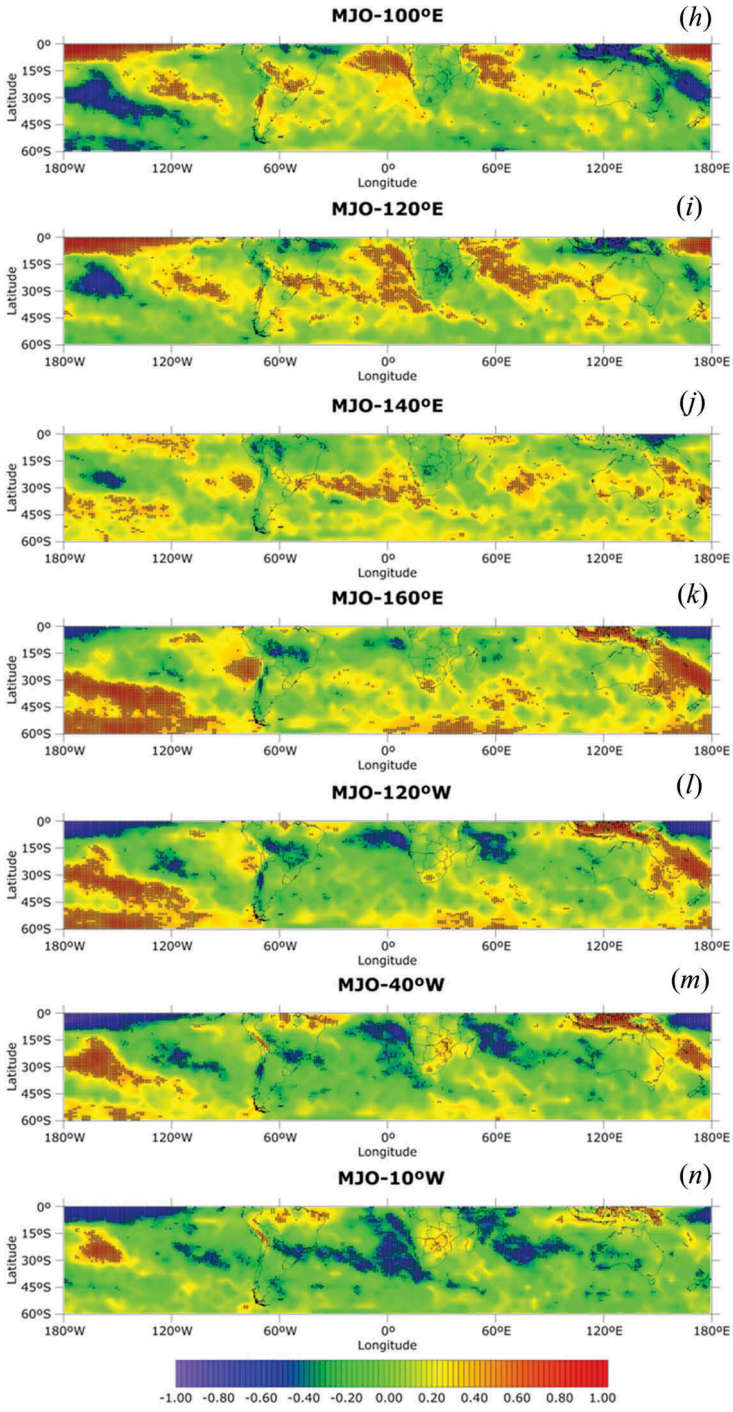

means retrieved from http://jisao.washington.edu/pdo/PDO.latest), the quasi-biennial oscillation (QBO, (Baldwin et al. 2001); monthly means retrieved from http://www.esrl.noaa.gov/psd/data/correlation/qbo.data), the SOI (Ropelewski and Jones (1987); monthly

means retrieved from the CPC database are described earlier) and the Madden–Julian oscillation (MJO, Zhang (2005); data available in pentads at 10 different longitudes retrieved from http://www.cpc.ncep.noaa.gov/products/precip/CWlink/daily_mjo_index/proj_norm_order.ascii and monthly means derived thereof).

The correlations field for the DMI shows a dipole in its region of influence, i.e. the tropical IO. The count of significant values for ρ is 1823. Positive (negative) coefficients indicate not only that the correlated anomalies are in direct (indirect) relationship, i.e. that during a positive phase of the DMI LER values are above (below) their mean in the western (eastern) tropical IO in concordance with a westward shift of precipitation (Saji et al. 1999), but also that the more positive (negative) the LER anomalies are in the western (eastern) tropical IO the stronger the positive phase of the DMI. The converse situation takes place for a negative polarity of the DMI. Besides the local effect (i.e. considering significant ρ values beyond the tropical IO) a positive polarity of the DMI has a negative effect in reflectivity (i.e. lesser cloudiness) in spots of the tropical central Pacific and eastern Australia and a positive effect elsewhere in the globe, most notably in the eastern subtropical Pacific and in the south-eastern IO, south of Australia. Moreover, a significant positive signal is also present in the central region of Argentina, the only such result for all the analysed indices within the timescales involved.

The PDO is the only circulation index used in this article that has contributions from extra-tropical latitudes. The count of significant ρ points is 2015. They show that a positive polarity of the PDO is matched by an increase in cloudiness across the tropical central-to-western Pacific, whereas a decrease in cloudiness extends from the north-west to the south-east of the Pacific's basin, in the southernmost portion of the IO, over the northernmost latitudes of South America, and along a horseshoe over Africa. As to the QBO, it is a process that takes place mostly in the equatorial stratosphere (the index used here is a zonal average of zonal winds at 30 hPa) and is related to low-latitude convection (Baldwin et al. 2001). Considering the small influence the QBO has in the troposphere (Baldwin et al. 2001) the low count of significant ρ values (590) for the correlation between QBO anomalies and LER ones is not unexpected. Nevertheless, they are mostly negative, and most of them are located in the subtropical IO.

The correlations map linking yearly LER anomalies with the SOI ones has 2731 significant points. Significant negative values of ρ are mostly located over tropical and subtropical oceans, but they also take place in northern Bolivia and in the southern Andes. As expected, years with a net negative (positive) value of the SOI index, i.e. ENSO warm (cold) events, are associated to reflectivity values above (below) the average in the central tropical Pacific; similarly, high snow accumulation in the central Andes is expected during an ENSO warm event (Masiokas et al. 2006), thus increasing the LER values. On the other hand, significant positive values of ρ extend from the maritime continent south-eastwards along the Pacific, and they also occur over southern Africa and northern Brazil, in compliance with Nicholson and Entekhabi (1986) and Ropelewski and Halpert (1989) an references therein, respectively, and over the Bolivian and the Peruvian Andes, by contrast to northern Bolivia. The remarkable opposite sign in the correlation values in the latter case is also in agreement with the literature (Ronchail and Gallaire 2006).

Figures 4(*a*)–(*n*) also present the correlation maps for the 10 different longitudes the MJO indices are given at. They are provided for the sake of completeness; it is not necessary to perform an analysis for all of them since there are similarities among the maps by virtue of the phases the MJO takes on along a tropical circle of latitude (Zhang 2005). This point is illustrated with a comparison between the maps that have the greatest number of significant correlation values, namely 70° E (with 3474 points out of 17,280 in the entire domain, or 20% of it) and 160° E (with 3261). The regions of significance in both maps are almost the same but the values of ρ have opposite sign. The pattern for 70° E is inverted with respect to the SOI one. Recalling that the SOI is negative for an ENSO warm event, this is a manifestation of the known positive ENSO/MJO relationship (Zhang 2005, and references therein). On the other hand, the two maps with the lowest number of significant points correspond to the MJO at 140° E (1364) and 10° W (2265). They also resemble the features of the 70° E and 160° E maps in that they have common regions with significant values of ρ but with opposite sign.

Given that most of the indices are of tropical nature, the correlation maps presented here may be seen as teleconnection patterns (see, e.g. Mo and White (1985)). Using LER anomalies as a diagnostic variable, they link the Tropics with the extra-Tropics in the SH. Implicit in these patterns is the fact that ρ calculated on the anomalies permit a bidirectional evaluation of trends, not necessarily linear, primarily at those regions where significance occurs and for the indices for which the highest absolute values of ρ were obtained.

4. Summary and concluding remarks

Annual UV LER anomalies in a region bounded by 0° S and 60° S within the period November 1978–November 2005 were presented and their trends estimated. With the exception of few regions where reflectivity may represent the contribution of both cloudiness and snow, trends in LER anomalies provided an evolution of total cloudiness within the study period. On average, the study region experienced a net increase in LER values of 0.78 RU decade^{-1}. If only significant trend values are considered the mean trend increases to 1.18 RU decade^{-1}. The region that showed the largest upward trend, up to 4 RU decade^{-1}, was located over the eastern Pacific, off the coasts of Chile and Peru, in a region with the frequent presence of stratocumulus. Despite the overall positive trend there were regions that yielded a negative one, most notably the tropical latitudes of South America and Africa. These results are in qualitative agreement with previous findings. The yearly zonal means also showed a positive trend at all latitudes, but significance occurred beyond 20° S only.

A novel contribution is the introduction of correlation maps between the LER anomalies and those of five different circulation indices, namely the DMI, the PDO, the QBO, the SOI, and the MJO at 10 latitudes. In particular, the Spearman's correlation, acting on the ranks of the time series rather than on their raw values, was implemented. Unlike Pearson's correlation, the methodology addresses the existence of a monotonic function, not necessarily linear, that relates the correlated variables. The index with the highest number of significant ρ values (3474 out of 17,280, or 20% of the domain) is the MJO at 70° E. By contrast, and likely related to the fact that the index is mostly

representative of the equatorial stratosphere, the QBO has the lowest number of significant correlation points.

This first study, entirely devoted to the SH, has been carried out using TOMS UV LER data covering the 1978–2005 period. The analysis will be extended by examining different timescales and with the incorporation of more recent data from other TOMS-like sensors.

Acknowledgement

The authors would like to thank two anonymous reviewers for their comments and suggestions. This research was partly funded by CONICET PIP 2012-2014 0075, Agencia Nacional de Promoción Científica y Tecnológica PICT-2012-2927 and Ministerio de Defensa PIDDEF 26/2014 grants.

Disclosure statement

No potential conflict of interest was reported by the authors.

Funding

This research was partly funded by CONICET PIP 2012-2014 0075, Agencia Nacional de Promoción Científica y Tecnológica PICT-2012-2927 and Ministerio de Defensa PIDDEF 26/2014 grants.

ORCID

Adrián E. Yuchechen http://orcid.org/0000-0002-3823-2291
S. Gabriela Lakkis http://orcid.org/0000-0001-7562-8204
Pablo O. Canziani http://orcid.org/0000-0003-0460-5544

References

Ambrizzi, T., E. B. De Souza, and R. S. Pulwarty. 2004. "The Hadley and Walker Regional Circulations and Associated ENSO Impacts on South American Seasonal Rainfall." In *The Hadley Circulation: Present, past and Future*, edited by H. F. Diaz and R. S. Bradley, 203–235. Dordrecht: Kluwer. doi:10.1007/978-1-4020-2944-8.

Ashkenazy, Y., H. Yizhaq, and H. Tsoar. 2012. "Sand Dune Mobility under Climate Change in the Kalahari and the Australian Deserts." *Climatic Change* 112 (3): 901–923. doi:10.1007/s10584-011-0264-9.

Baldwin, M. P., L. J. Gray, T. J. Dunkerton, K. Hamilton, P. H. Haynes, W. J. Randel, J. R. Holton, et al. 2001. The Quasi-Biennial Oscillation. *Reviews of Geophysics* 39 (2): 179–229. DOI:10.1029/1999RG000073.

Bornman, J. F., P. W. Barnes, S. A. Robinson, C. L. Ballaré, S. D. Fliont, and M. M. Caldwell. 2015. "Solar Ultraviolet Radiation and Ozone Depletion-Driven Climate Change: Effects on Terrestrial Ecosystems." *Photochemical & Photobiological Sciences* 14: 88–107. doi:10.1039/C4PP90034K.

Boucher, O., D. Randall, P. Artaxo, C. Bretherton, G. Feingold, P. Forster, V.-M. Kerminen, et al. 2013. "Clouds and Aerosols." In *Climate Change 2013: The Physical Science Basis. Contribution of Working Group I to the Fifth Assessment Report of the Intergovernmental Panel on Climate Change*, edited by T. F. Stocker, D. Qin, G.-K. Plattner, M. Tignor, S. K. Allen, J. Boschung, A. Nauels, Y. Xia, V. Bex, and P. M. Midgley, 571–657. New York, USA: Cambridge University Press.

Buchard, V., C. Brogniez, F. Auriol, B. Bonnel, J. Lenoble, A. Tanskanen, B. Bojkov, and P. Veefkind. 2008. "Comparison of OMI Ozone and UV Irradiance Data with Ground-Based Measurements at Two French Sites." *Atmospheric Chemistry and Physics* 8: 4517–4528. doi:10.5194/acp-8-4517-2008.

Cess, R. D., and P. M. Udelhofen. 2003. "Climate Change during 1985–1999: Cloud Interactions Determined from Satellite Measurements." *Geophysical Research Letters* 30 (1): 1019. doi:10.1029/2002GL016128.

Damiani, A., R. R. Cordero, S. Cabrera, M. Laurenza, and C. Rafanelli. 2014. "Cloud Cover and UV Index Estimates in Chile from Satellite-Derived and Ground-Based Data." *Atmospheric Research* 138: 139–151. doi:10.1016/j.atmosres.2013.11.006.

Den Outer, P. N., A. Van Dijk, H. Slaper, A. V. Lindfors, H. De Backer, A. F. Bais, U. Feister, T. Koskela, and W. Josefsson. 2012. "Applying Spaceborne Reflectivity Measurements for Calculation of the Solar Ultraviolet Radiation at Ground Level." *Atmospheric Measurement Techniques* 5: 3041–3054. doi:10.5194/amt-5-3041-2012.

Eastman, R., and S. G. Warren. 2013. "A 39-Year Survey of Cloud Changes from Land Stations Worldwide 1971-2009: Long-Term Trends, Relation to Aerosols, and Expansion of the Tropical Belt." *Journal of Climate* 26: 1286–1303. doi:10.1175/jcli-d-12-00280.1.

Eck, T. F., P. K. Bhartia, P. H. Hwang, and L. L. Stowe. 1987. "Reflectivity of Earth's Surface and Clouds in Ultraviolet from Satellite Observations." *Journal of Geophysical Research* 92 (D4): 4287–4296. doi:10.1029/jd092id04p04287.

Eckermann, S. D., and P. Preusse. 1999. "Gobal Measurements of Stratospheric Mountain Waves from Space." *Science* 286 (139): 1534–1537. doi:10.1126/science.286.5444.1534.

Häder, D.-P., H. D. Kumar, R. C. Smith, and R. C. Worrest. 2003. "Aquatic Ecosystems: Effects of Solar Ultraviolet Radiation and Interactions with Other Climatic Change Factors." *Photochemical & Photobiological Sciences* 2: 39–50. doi:10.1039/B211160H.

Hahn, C. J., and S. G. Warren. 1999. *Extended Edited Synoptic Cloud Reports from Ships and Land Stations over the Globe, 1952–1996*. Oak Ridge, TN: Carbon Dioxide Information Analysis Center. doi:10.3334/CDIAC/cli.ndp026c.

Herman, J., M. T. DeLand, L.-K. Huang, G. Labow, D. Larko, S. A. Lloyd, J. Mao, W. Qin, and C. Weaver. 2013. "A Net Decrease in the Earth's Cloud, Aerosol, and Surface 340 Nm Reflectivity during the past 33 Yr (1979-2011)." *Atmospheric Chemistry and Physics* 13: 8505–8524. doi:10.5194/acp-13-8505-2013.

Herman, J. R., P. K. Bhartia, A. J. Krueger, R. D. McPeters, C. G. Wellemeyer, C. J. Seftor, G. Jaross, et al. 1996. *Meteor–3 Total Ozone Mapping Spectrometer (TOMS) Data Products User's Guide*. Greenbelt, MD: National Aeronautics and Space Administration.

Herman, J. R., and E. A. Celarier. 1997. "Earth Surface Reflectivity Climatology at 340–380 Nm from TOMS Data." *Journal of Geophysical Research* 102 (D23): 28003–28011. doi:10.1029/97JD02074.

Herman, J. R., G. Labow, N. C. Hsu, and D. Larko. 2009. "Changes in Cloud and Aerosol Cover (1980–2006) from Reflectivity Time Series Using Seawifs, N7-TOMS, EP-TOMS, SBUV-2, and OMI Radiance Data." *Journal of Geophysical Research* 114: D01201. doi:10.1029/2007JD009508.

Hoel, P. G. 1984. *Introduction to Mathematical Statistics*. LaVergne TN, USA: Wiley.

Hoskins, B. J., and K. I. Hodges. 2005. "A New Perspective on Southern Hemisphere Storm Tracks." *Journal of Climate* 18: 4108–4129. doi:10.1175/JCLI3570.1.

Inatsu, M., and B. J. Hoskins. 2004. "The Zonal Asymmetry of the Southern Hemisphere Winter Storm Track." *Journal of Climate* 17: 4882–4892. doi:10.1175/JCLI-3232.1.

Kidson, J. W. 1999. "Principal Modes of Southern Hemisphere Low-Frequency Variability Obtained from NCEP–NCAR Reanalyses." *Journal of Climate* 12: 2808–2830. doi:10.1175/1520-0442(1999)012<2808:PMOSHL>2.0.CO;2.

Kondratyev, K. Y., and C. Varotsos. 1995. "Atmospheric Greenhouse Effect in the Context of Global Climate Change." *Il Nuovo Cimento C* 18 (2): 123–151. doi:10.1007/BF02512015.

Kuang, Z. K., and Y. L. Yung. 2000. "Reflectivity Variations of the Peru Coast: Evidence for Indirect Effect of Anthropogenic Sulfate Aerosols in Clouds." *Geophysical Research Letters* 27 (16): 2501–2504. doi:10.1029/2000GL011376.

Labow, G. J., J. R. Herman, L.-K. Huang, S. A. Lloyd, M. T. DeLand, W. Qin, J. Mao, and D. E. Larko. 2011. "Diurnal Variation of 340 Nm Lambertian Equivalent Reflectivity Due to Clouds and Aerosolos over Land and Oceans." *Journal of Geophysical Research* 116: D11202. doi:10.1029/2010JD014980.

Lamb, P. J., and R. A. Peppler. 1987. "Norht Atlantic Oscillation: Concept and Application." *Bulletin of the American Meteorological Society* 68 (10): 1218–1225. doi:10.1175/1520-0477(1987)068<1218:NAOCAA>2.0.CO;2.

Liang, S., K. Wang, X. Zhang, and M. Wild. 2010. "Review on Estimation of Land Surface Radiation and Energy Budgets from Ground Measurement, Remote Sensing and Model Simulations." *IEEE Journal of Selected Topics in Applied Earth Observations and Remote Sensing* 3 (3): 225–240. doi:10.1109/JSTARS.2010.2048556.

Mantua, N. J., S. R. Hare, Y. Zhang, J. M. Wallace, and R. C. Francis. 1997. "A Pacific Interdecadal Climate Oscillation with Impacts on Salmon Production." *Bulletin of the American Meteorological Society* 78 (6): 1069–1079. doi:10.1175/1520-0477(1997)078<1069:APICOW>2.0.CO;2.

Masiokas, M. H., R. Villalba, B. H. Luckman, C. Le Quesne, and J. C. Aravena. 2006. "Snowpack Variations in the Central Andes of Argentina and Chile, 1951– 2005: Large-Scaleatmospheric Influences and Implications for Water Resources in the Region." *Journal of Climate* 19: 6334–6352. doi:10.1175/JCLI3969.1.

McClain, C. R., E. J. Ainsworth, R. A. Barnes, R. E. Eplee Jr., F. S. Patt, W. D. Robinson, M. Wang, and S. W. Bailey. 2000. "Volume 9, Seawifs Postlaunch Calibration and Validation Analyses, Part 1." In *Seawifs Postlaunch Technical Report Series*, eds S. B. Hooker, E. R. Firestone, and M. D. Greenbelt. Greenbelt, MD: NASA Goddard Space Flight Center.

McPeters, R. D., P. K. Bhartia, A. J. Krueger, J. R. Herman, B. M. Schlesinger, C. G. Wellemeyer, C. J. Seftor, et al. 1996. *Nimbus–7 Total Ozone Mapping Spectrometer (TOMS) Data Products User's Guide*. Greenbelt, MD: National Aeronautics and Space Administration.

McPeters, R. D., P. K. Bhartia, A. J. Krueger, J. R. Herman, C. G. Wellemeyer, C. J. Seftor, G. Jaross, et al. 1998. *Earth Probe Total Ozone Mapping Spectrometer (TOMS) Data Products User's Guide*. Greenbelt, MD: National Aeronautics and Space Administration.

Mo, K. C., and G. H. White. 1985. "Teleconnections in the Southern Hemisphere." *Monthly Weather Review* 113: 22–37. doi:10.1175/1520-0493(1985)113<0022:TITSH>2.0.CO;2.

Nappo, C. 2002. ""Terrain-Generated Gravity Waves." Chap. 3." In *An Introduction to Atmospheric Gravity Waves,* edited by R. Dmowska, J. R. Holton and H. Thomas Rossby. San Diego, CA: Associated Press.

Nicholson, S. E., and D. Entekhabi. 1986. "The Quasi-Periodic Behavior of Rainfall Variability in Africa and Its Relationship to the Southern Oscillation." *Archives for Meteorology, Geophysics, and Bioclimatology* A34: 311–348. doi:10.1007/BF02257765.

Norris, J. R. 2005. "Trends in Upper Level Caloud Cover and Surface Divergence over the Tropical Indo Pacific Ocean between 1952 and 1997." *Journal of Geophysical Research* 110: D21110. doi:10.1029/2005JD006183.

Ozone Monitoring Instrument (OMI) Algorithm Theoretical Basis Document, Volume III: Clouds, Aerosols, and Surface UV Irradiance. 2002. August. http://eospso.gsfc.nasa.gov/sites/default/files/atbd/ATBD-OMI-03.pdf

Ozone Monitoring Instrument (OMI) User's Guide. 2012. The OMI Team. January 5. http://disc.sci.gsfc.nasa.gov/Aura/additional/documentation/README.OMI_DUG.pdf

Peixoto, J. P., and A. H. Oort. 1992. *Physics of Climate*. New York: Springer-Verlag.

Philander, S. G. 1989. *El Niño, La Niña, and the Southern Oscillation*. San Diego CA, USA: Academic Press.

Pinedo Vega, J. L., C. Ríos Martínez, F. Mireles García, V. M. García Saldívar, J. I. Dávila Rangel, and A. R. Salazar Román. 2014. "Trend of Total Column Ozone over Mexico from TOMS and OMI Data (1978-2013)." *Atmósfera* 27 (3): 251–260. doi:10.1016/S0187-6236(14)71114-2.

Ronchail, J., and R. Gallaire. 2006. "ENSO and Rainfall along the Zongo Valley (Bolivia) from the Altiplano to the Amazon Basin." *International Journal of Climatology* 26: 1223–1236. doi:10.1002/(ISSN)1097-0088.

Ropelewski, C. F., and M. S. Halpert. 1989. "Precipitation Patterns Associated with the High Index Phase of the Southern Oscillation." *Journal of Climate* 2: 268–284. doi:10.1175/1520-0442(1989)002<0268:ppawth>2.0.co;2.

Ropelewski, C. F., and P. D. Jones. 1987. "An Extension of the Tahiti–Darwin Southern Oscillation Index." *Monthly Weather Review* 115: 2161–2165. doi:10.1175/1520-0493(1987)115<2161:aeotts>2.0.co;2.

Rossow, W. B., and R. A. Schiffer. 1999. "Advances in Understanding Clouds from ISCCP." *Bulletin of the American Meteorological Society* 80: 2261–2287. doi:10.1175/1520-0477(1999)080<2261:aiucfi>2.0.co;2.

Saji, H. H., B. N. Goswami, P. N. Vinayachandran, and T. Yamagata. 1999. "A Dipole Mode in the Tropical Indian Ocean." *Nature* 401: 360–363. doi:10.1038/43854.

Schoterer, U., M. Grosjean, W. Stichler, P. Ginot, C. Kull, H. Bonnaveira, B. Francou, et al. 2003. Glaciers and Climate in the Andes between the Equator and 30°S: What is Recorded under Extreme Environmental Conditions? *Climatic Change* 59 :157–175. Doi:10.1023/A:1024423719288

Spencer, R. W., and W. D. Braswell. 2008. "Potential Biases in Feedback Diagnosis from Observational Data: A Simple Model Demonstration." *Journal of Climate* 21: 5624–5628. doi:10.1175/2008JCLI2253.1.

Spencer, R. W., and W. D. Braswell. 2011. "On the Misdiagnosis of Surface Temperature Feedbacks from Variations in Earth's Radiant Energy Balance." *Remote Sensing* 3: 1603–1613. doi:10.3390/rs3081603.

Stokes, S., G. Haynes, D. S. G. Thomas, J. L. Horrocks, M. Higginson, and M. Malifa. 1998. "Punctuated Aridity in Southern Africa during the Last Glacial Cycle: The Chronology of Linear Dune Construction in the Northeastern Kalahari." *Palaeogeography, Palaeoclimatology, Palaeoecology* 137: 305–322. doi:10.1016/s0031-0182(97)00106-5.

Stowe, L. L., H. Y. M. Yeh, T. F. Eck, C. G. Wellemeyer, and H. L. Kyle; the Nimbus-7 Cloud Data Processing Team. 1989. "Nimbus-7 Global Cloud Climatology. Part II: First Year Results." *Journal of Climate* 2: 671–709. doi:10.1175/1520-0442(1989)002<0671:ngccpi>2.0.co;2.

Trenberth, K. E., and J. T. Fasullo. 2009. "Global Warming Due to Increasing Absorbed Solar Radiation." *Geophysical Research Letters* 36: L07706. doi:10.1029/2009GL037527.

Varotsos, C. A. 2013. "The Global Signature of the ENSO and SST-Like Fields." *Theoretical and Applied Climatology* 113: 197–204. doi:10.1007/s00704-012-0773-0.

Varotsos, C. A., I. N. Melnikova, A. P. Cracknell, C. Tzanis, and A. V. Vasilyev. 2014. "New Spectral Functions of the Near-Ground Albedo Derived from Aircraft Diffraction Spectrometer Observations." *Atmospheric and Chemistry Physics* 14: 6953–6965. doi:10.5194/acp-14-6953-2014.

Von Schuckmann, K., M. D. Palmer, K. E. Trenberth, A. Cazenave, D. Chambers, N. Champollion, J. Hansen, et al. 2016. "An Imperative to Monitor Earth's Energy Imbalance." *Nature Climate Change* 6: 138–144. doi:10.138/nclimate2876.

Wilks, D. S. 2006. "Review of Probability." Chap. 2. 2nd. *Statistical Methods in the Atmospheric Sciences*. Burlington, MA: Academic Press.

Yasunari, T. 1977. "Stationary Waves in the Southern Hemisphere Mid-Latitude Zone Revealed from Average Brightness Charts." *Journal of the Meteorological Society of Japan* 55 (3): 274–285.

Zhang, C. 2005. "Madden-Julian Oscillation." *Reviews of Geophysics* 43 (RG2003). doi:10.1029/2004RG000158.